The Journal of Physical Chemistry B

 VOLUME 103, NUMBER 28, JULY 15, 1999

LETTERS

Origin of Photovoltage and Photocurrent in the Nanoporous Dye-Sensitized Electrochemical Solar Cell

Klaus Schwarzburg and Frank Willig*,†

Hahn-Meitner-Institut, Glienicker Strasse 100, 14109 Berlin, Germany

Received: January 26, 1999; In Final Form: April 28, 1999

The essential role of the dark equilibrium potential is discussed for charge separation and the photovoltaic functioning of the title cell. A quantitative model is presented for the potential distribution in the sponge-type title cell. The unique screening process for the photogenerated electrons is discussed that facilitates their extremely long lifetime since the screening ions cannot function as recombination centers. A general analogy is pointed out for the photovoltaic functioning of the sponge-type electrochemical solar cell and of a conventional single-crystal solid-state solar cell.

I. Introduction

This letter addresses the nanoporous dye-sensitized electrochemical solar cell,[1,2] in particular the dark equilibrium potential and its role in the photovoltaic functioning of this sponge-type cell. In the presently available models for the latter process,[3,4] the sponge-type cell has been treated as continuous medium. The actual structure of the nanoporous TiO_2 network is neglected. The latter is immersed in an electrolyte of high ionic strength. Photocurrent transients[5,6] show extremly slow diffusion of screened charge carriers and appear to be compatible with the assumption of an effective continuous medium. However, the diffusion coefficient is much smaller than for electrons in TiO_2 single crystals. The mechanism of charge separation has remained unclear in the above treatments of the sponge-type cell. It is shown in this letter that the equilibrium dark potential is an essential feature for the photovoltaic functioning of the cell. Location and spatial extension of the dark potential drop is discussed with a quantitative model, making use of a minimum geometrical representation of the nanoporous TiO_2 network. The unique nature of the screening process for the photogenerated electrons in the sponge-type cell is explained, as well as their final separation from the ionic screening charges in the dark potential drop. The latter process gives rise to the photopotential and generates the photocurrent in the cell.

II. Equilibrium Potential in the Dark

Figure 1a shows a simplified scheme of the sintered colloidal TiO_2 network that is immersed in an electrolytic solution of high ionic strength (typically 0.3 M LiI, 0.03 M I_2 dissolved in acetonitrile[7]) and attached on one side to a planar highly n-conducting SnO_2:F layer.[8] Gregg et al.[9] have advanced the qualitative notion that because of screening by the high ionic concentration in the electrolyte an externally applied potential should be confined to sections of the TiO_2 network that are adjacent to the conducting SnO_2:F electrode. However, the existence of an equilibrium dark potential in this cell has been denied by these authors.

First, the existence of the equilibrium dark potential will be discussed. According to general thermodynamic rules, a difference in the chemical potential of two different contact materials will be balanced upon contact formation via the

† Parts of this letter have been presented as an invited talk at the Spring Meeting of the German Physical Society, March 1998, Regensburg, Germany.

10.1021/jp990312s CCC: $18.00
Published on Web 06/24/1999

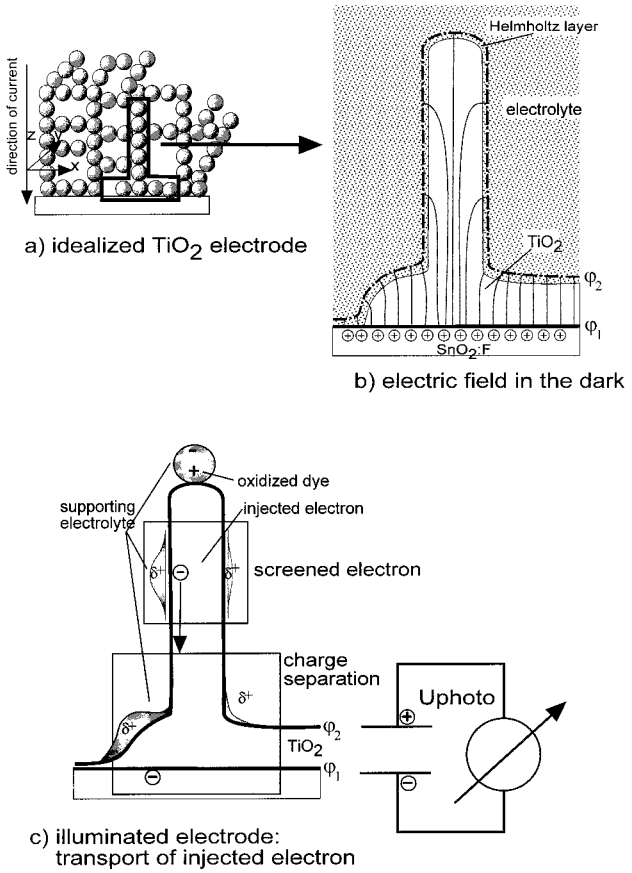

Figure 1. (a) Schematic model of the TiO_2 network. (b) Illustration of electric field in the dark. (c) Screening and separation of the photogenerated electron from the screening charge.

exchange of charges and/or formation of a dipole layer such that a corresponding potential drop is set up that leads to a constant electrochemical potential across the interface. The resulting spatial separation of opposite charges defines a capacitive element in the cell. A specific example is that of contact formation between a metal or a highly conductive semiconductor, i.e., the Pt counter electrode and SnO_2:F layer in the present cell, and an electrolyte that contains a redox couple and salt of high ionic strength. The corresponding equilibrium potential drop over the Helmholtz layer is well documented.[10] Insertion of the TiO_2 network between the electrolyte and the electrode plate (Figure 1a) will modify the spatial distribution but not the magnitude of the equilibrium potential drop. In the case where the TiO_2 network can be considered an insulator, the potential distribution will follow that shown in Figures 1b and 2. To set up the equilibrium potential in the cell it is not required that charge is passing through the TiO_2 network in the dark. It is sufficient that it can pass through a resistance or a conducting wire[11] that connects the SnO_2:F electrode with the Pt counter electrode, the latter being in direct contact with the redox electrolyte. This latter mode of charge exchange appears realistic for the cell in view of the more than 1 eV energy difference between the redox potential in the solution and the lower conduction band edge of anatase TiO_2. It is important to note that the magnitude of the equilibrium potential drop is controlled by the difference between the Fermi level in the SnO_2:F electrode and the redox potential of the I^-/I_2 redox couple in the solution before contact formation.

To understand the photovoltaic functioning of the title cell it is important to know the spatial distribution of the equilibrium potential drop. It it is helpful to define here a minimum element

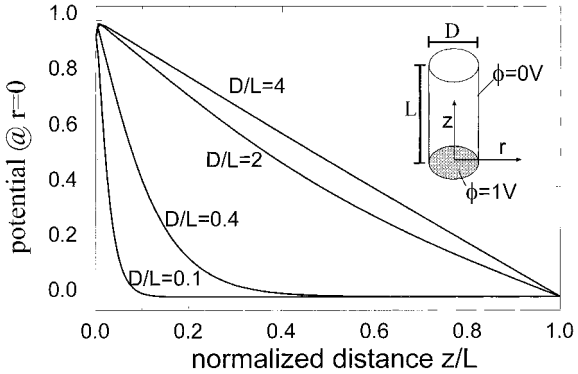

Figure 2. Electric potential along the rotational axis of a hollow conducting cylinder, where the base plate is at a different potential than all the other surface elements (minimum electrostatic model for the nanoporous TiO_2 network immersed into a strong electrolyte).

of the colloidal network. This is a chain of colloids extending in perpendicular direction from the SnO_2:F base into the electrolytic solution (Figure 1a). To obtain a quantitative solution for the potential, the above element is further simplified to a hollow cylinder with conducting walls, where one base plate is kept at a given potential and the potential of the remaining surface area is defined at zero. This base plate represents the SnO_2:F contact and the remaining surface area the contact area of TiO_2 with the highly conducting electrolyte. In this simple approximation we neglect the small gap corresponding to the Helmholtz layer. There is an analytical solution to this electrostatic problem, i.e., to the Laplace equation, for the absence of point charges inside of the hollow cylinder.[12] The solution is illustrated in Figure 2, where the potential along the rotational axis of the cylinder is plotted for different values of the ratio diameter (D)/length (L). The well-known potential in a parallel plate capacitor, i.e., a linear drop of the potential over the length of the cylinder, is recovered for $D/L > 4$. On the other hand, for $D/L \ll 4$ most of the potential drop occurs within a distance $d < D$. Values $D/L = 0.001-0.01$ correspond to typical dimensions of the nanoporous sponge-type TiO_2 network in the cell. Note that the cylinder corresponds to a chain of sintered colloids (Figure 1a). Typically, the diameter can vary between one (10−20 nm) and say 5 colloidal diameters. The length of the cylinder is simply of the order of the total thickness of the film formed by the collidal network, i.e., typically 10 μm. The quantitative model predicts that the total potential drop occurs in such a case within a distance that extends from the cylinder base, i.e., the SnO_2:F electrode, over a few 10 nm, i.e., over only one or two colloidal diameters. Thus, most of the TiO_2 network remains virtually field free. This spatial qualitative distribution of the equilibrium voltage drop will hold true independent of the intricacy of the actual colloidal network as long as its basic dimensions are not altered significantly.

III. Transport and Separation of Photogenerated Electrons from Their Screening Charge

Figure 1c illustrates screening due to the high ionic strength in the electrolyte. Both charges, i.e., the electron injected into the TiO_2 network and the positive counter charge left behind on the dye molecule, are screened effectively over the diameter of the ionic cloud due to 0.5 LiI, i.e., over a few nm. Also under sunlight the concentration of electrons photoinjected into the TiO_2 network and their positive countercharges remains much smaller than the concentration of ions in the surrounding electrolyte. The major part of this screening process is controlled by the relaxation time of the ions in solution, i.e., nanoseconds.[13]

Additional much faster partial screening occurs in polar solvents on the femtosecond time scale.[14,15] Very fast partial screening corresponds to the optical dielectric constant of anatase TiO_2. The latter material contributes additional slower screening that corresponds to the static dielectric constant. The initially photogenerated electron−hole pair, i.e., the oxidized dye and the injected electron, are transformed via these screening processes into essentially neutral species as illustrated in Figure 1c. The injected electron moves about along with its screening charge as an essentially neutral particle in the field free TiO_2 network. The essential advantage of the electrolytic screening process is its independence from recombination events. The redox potential of the Li^+ ions[16] lies at −3 V (NHE), about 2 eV higher than the redox potential in the range of > −1 V (NHE) of the electrons in the TiO_2 network.[17] It appears extremely difficult to incorporate a corresponding screening process into a solid-state cell. The majority carriers that provide the screening charge for a photogenerated minority carrier in a solid-state cell are very efficient reaction partners for recombination. The diffusional motion of the screened photogenerated electrons in the 3-dimensional TiO_2 network in the present cell bears some gross resemblence to the diffusional motion of screened photogenerated minority carriers in the bulk of a single-crystal solid-state solar cell.[18−21] However, the effective diffusion constant for the screened photogenerated electron in the present cell is between 6 and 9 orders of magnitude smaller than in the bulk of a single-crystal solid-state cell. In the present cell this diffusion constant cannot be identified with that of the ions in solution. Debey relaxation of the ionic cloud rather than the actual diffusion of ions is connected with the motion of the injected electron. A change in the viscosity of the electrolyte did not affect the shape or time scale of the photocurrent transients in the cell.[22] The slow, i.e., ms, transport in the present cell is controlled by trapping and detrapping events.[23,11] Fast trapping of the injected electrons is expected to help in building up the screening charge before geminate recombination can take place. The influence of the latter is also greatly diminished by the 3-dimensional nature of the TiO_2 network as opposed to a 1-dimensional system.[24] It has been reported that the oxidized dye molecule transfers the positive charge to I^- on the time scale of 100 ns.[25] This shifts the recombination process from geminate and nongeminate events to alien recombination,[26] and the latter controls the recombination losses in the cell.[27,28] The slowness of the decisive alien recombination process that involves the complete interface electrolyte/TiO_2 network must be due to the small concentration of the actual active oxidized redox species at this interface. The latter species has not yet been identified. It is most likely not the species I_3^- of the electrolytic bulk solution but a species derived from the latter via bond splitting. The photopotential is built up in the cell by spatially separating the injected electrons from their screening charges (bottom of Figure 1c). This charge separation occurs because of the equilibrium potential drop discussed in section II above and is represented in the model as boundary condition for the diffusion process.[8−21] Accumulation of the photogenerated electrons in the SnO_2:F layer and of positive charges in the adjacent electrolyte leads to the photopotential. Thus, compensation of the equilibrium potential established in the dark (Figure 2b) sets the upper limit for the achievable photopotential.

A smaller modification of the above picture could arise if the conduction band of TiO_2 is located above that of SnO_2:F at this interface. Such a downhill step in the electron affinities at the interface can facilitate electron−hole pair separation.

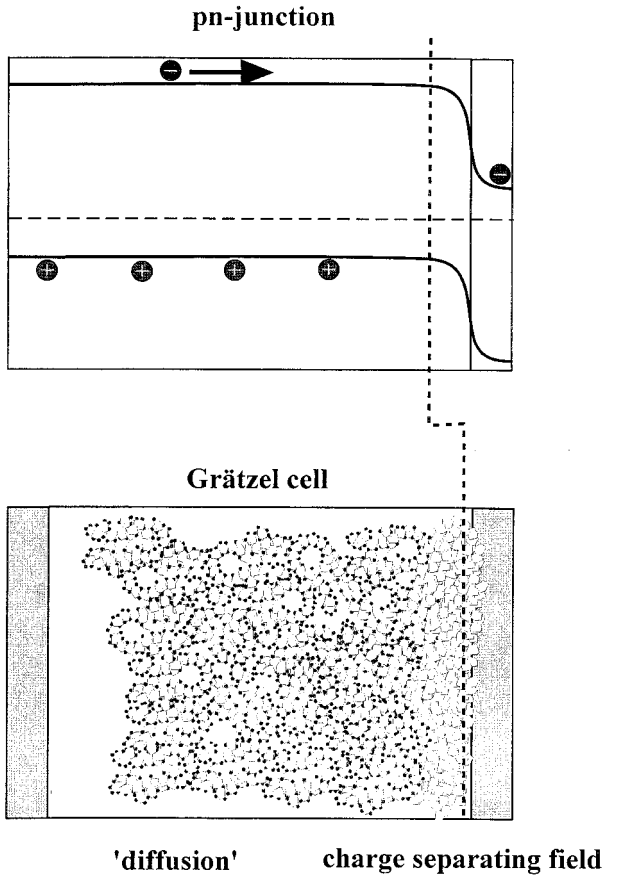

Figure 3. General analogy between the nanoporous dye-sensitized solar cell and a solid-state p−n junction solar cell.

However, it would not be sufficient for sustaining the so-called "kinetic model" in the title cell (compare the comment following ref 31).

IV. Experimental Support for the Model

The overall analogy in the photovoltaic functioning of the title cell and a conventional p−n junction solar cell[29] based on the above discussion is illustrated in Figure 3. Correspondingly, the current−voltage characteristics of the cell for the dark current,[30] for the photocurrent,[27,31,32] and the dependence of photopotential on light intensity[27,31,32] and on temperature[27] all show qualitative behavior similar to a solid-state solar cell. A capacitance of about 10 $\mu F/cm^2$ [36] was determined for the sponge-electrode which is of the order of magnitude expected for the Helmholtz capacitance in agreement with the model illustrated in Figures 1b and 2. A reliable direct experimental determination of the Fermi level in the SnO_2:F electrode before contact formation is not known to us. An estimate can be obtained from a related experimental system.[33] The difference between the latter value and the redox potential of the I^-/I_3^- redox system[34] is in qualitative agreement with the reported photopotential of the sponge-type cell in the range of 700 mV.[7,35] The SnO_2:F electrode contains a high concentration of fluoride and it is well-known that a layer of fluoride at the oxide surface can shift the Fermi level considerably upward, e.g., by 1 V,[38] The best way of determining the actual dark potential in the title cell is a direct measurement.[36] Photocurrent transients, measured in the sponge-type cell, have been ascribed to diffusional transport,[5,6] where the mobile photogenerated species can be identified with the screened photogenerated electron illustrated in Figure 1c. Except for a completely different time

scale, i.e., ms versus ps or ns, the origin of these photoinduced electrical transients is very similar to that of the photoinduced transients reported for the diffusional motion of screened photogenerated minority carriers in semiconductor single crystals,[18−21] where charge separation occurred in the dark potential drop established near the crystal surface. Photocurrent transients measured in the sponge-type TiO_2 cell[36] and photocurrent transients in related ZnO films[37] did not depend on blocking bias (positive of the flatband potential). This proves the absence of an electric field in the major part of the sponge-type cell (Figure 3).

Acknowledgment. The authors are grateful for financial support by the Joule III program.

References and Notes

(1) Vlachopoulos, N.; Liska, P.; Augustynski, J.; Grätzel, M. *J. Am. Chem. Soc.* **1988**, *110*, 1216.

(2) O'Regan, B.; Grätzel, M. *Nature* **1991**, *353*, 737

(3) Ferber, J.; Stangl, R.; Luther, J. *Sol. Energy Mater. Sol. Cells* **1998**, *53*, 29.

(4) Södergren, S.; Hagfeld, A.; Olsson, J.; Lindquist, S. E. *J. Phys. Chem* **1994**, *98*, 5552.

(5) Solbrand, A.; Lindstrom, H.; Rensmo, H.; Hagfeldt, A.; Lindquist, S. E.; Sodergren, S. *J. Phys. Chem. B* **1997**, *101*, 2514.

(6) Cao, F.; Oskam, G.; Meyer, G. J.; Searson, P. C. *J. Phys. Chem* **1996**, *100*, 17021.

(7) Nazeeruddin, M. K.; Kay, A.; Rodicio, I.; Humphrey-Baker, R.; Müller, E.; Liska, P.; Vlachopoulos, N.; Grätzel, M. *J. Am. Chem. Soc.* **1993**, *115*, 6382.

(8) Hartnagel, H. L.; Dawar, A. L.; Jain, A. K.; Jagadish, C. *Semiconducting Transparent Thin Films*, 1st ed.; Institute of Physics Publishing: Bristol, U.K., 1995.

(9) Zaban, A.; Meier, A.; Gregg, B. A. *J. Phys. Chem. B* **1997**, *101*, 7985.

(10) Equilibrium properties of electrified interfaces; In *Modern Aspects of Electrochemistry*; Bockris, J. O'M., Conway, B. E., Eds. Buttherworths: London, 1954; Vol. 1, p 103. Bockris J. O'M.; Reddy A. *Modern Electrochemistry*; Plenum Press: New York, 1970.

(11) Willig, F.; Burfeindt, B.; Schwarzburg, K.; Hannappel, T.; Storck, W. *Proc. Indian Acad. Sci.* **1997**, *109*, 415.

(12) Jackson, J. *Classical Electrodynamics*, 2nd ed; John Wiley & Sons: New York, 1975.

(13) Debye, P.; Falkenhagen, H. *Phys. Z.* **1928**, *29*, 401.

(14) Passino, S. A.; Nagasawa, Y.; Joo, T.; Fleming, G. R. *J. Phys. Chem.* **1997**, *101*, 725.

(15) Boeij, W. P.; Pshenichnikov, M. S.; Wiersma, D. A. *J. Phys. Chem.* **1996**, *100*, 11806.

(16) *CRC Handbook of Chemistry and Physics*, 64th ed.; CRC Press Inc.: Boca Raton, Florida, 1983.

(17) Redmond, G.; Fitzmaurice, D. *J. Phys. Chem.* **1993**, *97*, 1426.

(18) Willig, F. *Ber. Bunsen-Ges. Phys. Chem.* **1988**, *92*, 1312.

(19) Bitterling, K.; Willig, F. *J. Electroanal. Chem.* **1986**, *204*, 211.

(20) Bitterling, K.; Willig, F.; Decker, F. *J. Electroanal. Chem.* **1987**, *228*, 29.

(21) Schwarzburg, K.; Willig, F. *J. Phys. Chem. B* **1997**, *101*, 2451.

(22) Sommeling, P. M.; Rieffe, H. C.; Kroon, J. M.; van Roosmalen, J. A. M.; Schönecker, A.; Sinke, W. S. Spectral Response and Response Time of Nanocrystalline Dye-Sensitized TiO_2 Solar Cells; *14th European Photovoltaic Solar Energy Conference*, 1997.

(23) Schwarzburg, K.; Willig, F. *Appl. Phys. Lett.* **1990**, *58*, 2520.

(24) Blumen, A.; Klafter, J.; Zumhofen, G. *Models for Reaction Dynamics in Glasses*; D. Reidel Publishing Company: Dordrecht, The Netherlands, 1986.

(25) Haque, S. A.; Tachibana, Y.; Klug, D. R.; Durrant, J. R. *J. Phys. Chem. B* **1998**, *102*, 1745.

(26) Spin-Dependent Kinetics in Dye-Sensitized Charge-Carrier Injection into Organic Crystal Electrodes; In *Modern Aspects of Electrochemistry*; Conway, B. E., Bockris, J. O'M., White, R. E., Eds.; Plenum Press: New York, 1989; Vol. 19, p 359.

(27) Liu, Y.; Hagfeldt, A.; Xiao, X.-R.; Lindquist, S. E. *Sol. Energy Mater. Sol. Cells* **1998**, *55*, 267.

(28) Huang, Sy.; Kavan, L.; Exnar, I.; Grätzel, M. *J. Electrochem. Soc.* **1995**, *142*, L 142.

(29) Sze, S. M. *Physics of semiconductor devices*, 2nd ed.; John Wiley & Sons: New York, 1981.

(30) Stanley, A.; Verity, B.; Matthews, D. *Sol. Energy Mater. Sol. Cells* **1998**, *52*, 1.

(31) Huang, Sy.; Schlichthoerl, G.; Nozik, A.; Grätzel, M.; Frank, A. *J. Phys. Chem. B* **1997**, *101*, 2576. The referees have urged us to make a comment on a specific assumption that has appeared repeatedly in the literature on the title cell, where the generation of the photovoltage is assumed to occur in the absence of a dark potential, the so-called "kinetic model" (see below). Ref 31 has been quoted by the referees as an example. In ref 31 and several other papers dealing with the title cell, the establishment of a different chemical potential under light compared to the dark has been identified with the generation of a photopotential. However, in order to convert a chemical potential under light into a photopotential, it is of course necessary that electrons must be spatially separated from the corresponding positive charges, thus defining a capacitive element in the cell where the photovoltage appears (a different chemical potential can be established under light of course also in a homogeneous solution without generating any photopotential). According to the referees, the assumption of the so-called "kinetic model" is charge separation occurring automatically in the title cell (see above) in the absence of a dark equilibrium potential drop. Thus, the dark potential drop is considered irrelevant in the so-called "kinetic model". In the absence of a dark potential drop, the spatial separation of photogenerated electron−hole pairs requires a spatial gradient of consecutive electron affinities (or ionization energies), as it is found in the reaction center of photosynthesis. In the title cell, only one downhill step in electron affinities (conduction bands) could possibly occur at the interface between the last TiO_2 colloid and the SnO_2:F electrode, though to our knowledge this has not yet been experimentally verified. The photopotential of −0.8 V observed in the title cell, with the charge distribution described in this letter, would automatically imply in the absence of a dark equilibrium potential that the forward charge separating process would be slowed by the factor $\exp(0.8\ \mathrm{eV}/k_BT) = 10^{14}$ at room temperature. Translating this into a reaction time for the forward charge separating process at the interface, the latter would increase from say, e.g., initially a few 10 femtoseconds to several seconds in the presence of the complete photovoltage. However, for example, the fast rise time of the electrical phototransients in the title cell[36] is in clear contradiction to this consequence of the so-called "kinetic model". Neither has the experimental requirement of a spatial sequence of downhill steps in electron affinities been shown to exist in the title cell (a clear discussion of this case for semiconductors can be found in Würfel, P., *Physik der Solarzellen*; Spektrum Akademischer Verlag: Heidelberg, 1995; pp 111−113, Figure 6.14) nor has any decisive experimental observation been described in the literature that could be considered as strong support for the notion that the so-called "kinetic model" could really be operative in the title cell.

(32) Wahl, A.; Augustynski, J. *J. Phys. Chem. B* **1998**, *102*, 7820.

(33) Möllers, F.; Memming, R. *Ber. Bunsen-Ges Phys. Chem.* **1972**, *76*, 469.

(34) Datta, J.; Bhattacharya, A.; Kundu, K. K. *Bull. Chem. Soc. Jpn.* **1988**, *61*, 1735.

(35) Barbe, C. J.; Arendse, F.; Comte, P.; Jirousek, M.; Lenzmann, F.; Shklover, V.; Grätzel, M. *J. Am. Ceram. Soc.* **1997**, *80*, 3157.

(36) Meissner, B.; Schwarzburg, K.; Willig, F., to be published.

(37) Hoyer, P.; Weller, H. *J. Phys. Chem.* **1995**, *99*, 14096.

(38) Wang, C. M.; Mallouk, T. E. *J. Phys. Chem.* **1990**, *94*, 4276.